IJCRT.ORG ISSN : 2320-2882

INTERNATIONAL JOURNAL OF CREATIVE RESEARCH THOUGHTS (IJCRT)

An International Open Access, Peer-reviewed, Refereed Journal

Phytogenic Tio_2 Nanoparticles Synthesized From *Cichorium Intybus*: Antimicrobial Profiling And Wound Healing Potentially

[1]Devi Ougha, [2]Manjeet Kilhore, [3]Mantesh Yadav*

[1]Research scholar, [2]Research scholar, [3]Assistant Professor

[1]Department of Chemistry, School of Physical Sciences,

[1]Starex University, Gurugram, Haryana, 122413, India

Abstract

This study highlights the eco-friendly synthesis of titanium dioxide (TiO_2) nanoparticles (NPs) using *Cichorium intybus* leaf extract, followed by their detailed characterization and biomedical evaluation. The green-synthesized TiO_2 NPs were analyzed using XRD, SEM, FTIR, UV-Vis spectroscopy, and EDX techniques, confirming their purity, crystallinity, and structural integrity. FTIR identified functional groups stabilizing the nanoparticles, while XRD confirmed a predominant anatase phase with an average crystalline size of 10 nm. UV-Vis spectroscopy revealed a strong absorbance peak at 356 nm with a calculated bandgap energy of 3.48 eV. SEM images showed spherical morphology with minimal agglomeration, and EDX confirmed elemental composition. Biological evaluations revealed no significant antibacterial or antifungal activity against tested bacterial (*E. coli*, *S. marcescens*, *P. aeruginosa*) and fungal (*C. parapsilosis*, *T. asperellum*, *C. tropicalis*, *A. niger*) strains up to 1000 µg/well. Cytotoxicity analysis on L929 cell lines demonstrated slight cytotoxic effects, with an IC50 value of 944.1 µg/mL. A wound-healing assay showed promising results, with treated cells exhibiting a healing rate of 57.44% at 236.02 µg/mL compared to 42.17% in untreated cells after 24 hours. These findings emphasize the therapeutic potential of green-synthesized TiO_2 NPs, particularly in promoting wound healing, underscoring their significance in biomedical applications.

Keywords **:** Titanium metal , Nanoparticles, Ecofriendly, green synthesis

1. Introduction

The green synthesis of nanoparticles has garnered significant attention in recent years due to its simplicity, cost-effectiveness, and environmentally friendly nature.[1]–[6] These nanoparticles (NPs) exhibit unique properties such as enhanced shape, structure, and surface area, making them highly suitable for applications across diverse fields, including medicine, electronics, catalysis, food safety, and environmental remediation.[2], [5], [7]–[9] In particular, the development of green synthesis methodologies has become increasingly relevant to minimize hazardous waste, reduce the use of toxic chemicals, and align with sustainable practices.[10]–[13] Green synthesis processes emphasize the use of benign biological precursors and eco-friendly approaches that eliminate the need for high temperatures, pressures, or expensive reagents.[14]–[18] Among the various natural sources, *Cichorium intybus* (commonly known as chicory) leaves have been reported as an effective biological medium for stabilizing and controlling the size and morphology of nanoparticles.[19]–[22] Skin, as the largest organ in the human body, plays a vital role in maintaining homeostasis, sensory perception, and protecting against pathogens.[23] Injuries compromising the skin's integrity, such as burns, cuts, or chronic wounds, pose significant health challenges, particularly for patients with underlying conditions like diabetes, vascular dysfunction, or autoimmune diseases.[24]–[26] These infections can delay healing, worsen inflammation, and contribute to antimicrobial resistance (AMR), highlighting the need for alternative wound management strategies. Nanotechnology offers innovative solutions for wound healing and regenerative medicine.[27]–[30] Metallic nanoparticles, such as zinc oxide, gold, silver, and TiO_2, have emerged as promising candidates for wound healing applications.[24], [31]–[34] TiO_2 nanoparticles, in particular, exhibit antimicrobial, anti-inflammatory, and angiogenic properties, promoting cell proliferation and reducing scarring. Green-synthesized TiO_2 NPs, owing to their eco-friendly production process, further enhance their appeal for biomedical applications.[31], [32], [35], [36] This study investigates the synthesis and characterization of TiO_2 nanoparticles using *Cichorium intybus* leaf extract and their application in wound healing. By evaluating their antimicrobial efficacy, cytotoxicity, and wound healing potential, the research aims to explore cost-effective, eco-friendly, and clinically viable alternatives for addressing challenges in modern medicine, particularly in wound management. The findings of this study have broader implications for advancing nanotechnology-based therapies and contributing to sustainable healthcare solutions.

2. Experimental Section

2.1 Materials

All chemicals utilized in this study were procured from Spectrochem Pvt. Ltd., Loba Chemie Pvt Ltd and Sisco Research Laboratories (SRL) Pvt. Ltd. All chemicals were analytical grade and used as such in the study. Healthy and fresh leaves of *Cichorium incubus* were collected from local area VIII-Heraheri in the Pataudi district, Gurgaon (India) (Latitude: 28.30, Longitude: 76.76).

2.2 Methods and Instrumentation

2.2.1 Characterization of Sample

The FT-IR spectrum was recorded on a Thermo Scientific Nicolet Summit X FTIR Spectrometer, equipped with Everest ATR mode, at a resolution of 4 cm^{-1}. Pellets for FT-IR analysis were prepared by mixing KBr powder with the sample. The X-ray diffraction (XRD) analysis of the samples was conducted using an Empyrean X-ray Diffractometer from PANalytical B.V. Scanning electron microscopy (SEM) images of the nanoparticles were obtained using a HITACHI SU3500 instrument, with an acceleration voltage of 5-30 kV and magnification power ranging from 50x to 800,000x. The ultraviolet (UV) analysis of the samples was conducted using a Perkin Elmer LAMBDA 365 spectrophotometer, operating at a wavelength range of 200 nm to 800 nm. Thermal analysis was performed on a TA Instruments Discovery Series SDT650, with a scan rate of 15°C per minute, over a temperature range of 25°C to 1000°C.

2.2.2 Antibacterial Activity Assay

The antibacterial activity was assessed using the Zone of Inhibition Method (Kirby-Bauer method). Mueller-Hinton Agar (MHA) plates were inoculated by spreading 100 µL of bacterial culture (*S. marcescens*, *E. coli* (-ve), and *P. aeruginosa* (-ve)), prepared by adjusting to 0.5 McFarland Units (approximately 1.5×10^8 CFU/mL). Filter paper discs (5 mm, Whatman No. 1) loaded with 10 µL of various concentrations (0 to 100 mg/mL) of the samples were placed on the plates. A disc loaded with the solvent (DMSO) served as a vehicle control, while a Ciprofloxacin disc (10 µg) was used as a positive control. The plates were incubated at 37°C for 24 hours, and the diameter of the clear inhibition zones was measured and recorded.

2.2.3 Antifungal Activity Assay

The antifungal activity was also evaluated using the Zone of Inhibition Method (Kirby-Bauer method). Sabouraud Dextrose Agar (SDA) plates were inoculated with 100 µL of fungal cultures (*A. niger*, *C. parapsilosis*, *T. asperellum*, and *T. C. tropicalis*), prepared at 0.5 McFarland Units (approximately 1.5×10^8 CFU/mL). Filter paper discs (5 mm, Whatman No. 1) loaded with 10 µL of various concentrations (0 to 100 mg/mL) of the samples were placed on the plates. A solvent control (DMSO) and Amphotericin B (50 µg) served as controls. The plates were incubated at 37°C for 48 hours, and the clear inhibition zones were measured and recorded.

2.2.4 In Vitro Cytotoxicity Evaluation

The cytotoxicity of the samples was evaluated on L929 cell lines procured from National Centre for Cell Science (NCCS) Pune using the MTT assay. Cells (10,000 cells/well) were cultured in 96-well plates in Minimum Essential Medium (MEM) supplemented with 10% Fetal Bovine Serum (FBS) and 1% Penicillin-Streptomycin at 37°C with 5% CO_2 for 24 hours. The cells were treated with varying concentrations of the samples, prepared in incomplete MEM (without FBS). After 24 hours of incubation, an MTT solution (5 mg/mL) was added and incubated for 2 hours. The resulting formazan crystals were dissolved in 100 µL DMSO, and absorbance was recorded at 540 nm using an ELISA plate reader (iMark, Bio-Rad, USA). IC50 values were calculated using GraphPad Prism 6 software. Images were captured using an inverted microscope (Olympus EK2) equipped with a 10 MP Aptima CMOS camera.

2.2.5 Wound Healing Assay

L929 cells (10,000 cells/well) were cultured in 96-well plates in Dulbecco's Modified Eagle Medium (DMEM) supplemented with 10% FBS and 1% Penicillin-Streptomycin at 37°C with 5% CO_2. After 24 hours, a scratch was made using a 200 µL pipette tip. The cells were then treated with specific concentrations of the formulation. Images of the scratch area were captured at 0 and 24 hours using an inverted microscope (Olympus EK2) with a 10 MP Aptima CMOS camera. The gap area was analyzed using Image J software (NCBI) and presented graphically.

2.3 Synthetic Procedures

2.3.1 Preparation of *Cichorium incubus* leaves extract

Collected leaves of *Cichorium incubus* were washed thoroughly with tap water followed by distilled water to remove contaminants. A total of 50 g of leaves were weighed and transferred to a 500 mL beaker containing 100 mL of distilled water. The mixture was heated at 70°C for 1 hour and then filtered using filter paper. The obtained extract was stored away from dust and sunlight for further use in nanoparticle synthesis.

2.3.2 Synthesis of Nanoparticles

A 0.1 M solution of TiO_2 was prepared by dissolving amorphous titanium dioxide in ethanol. The leaves extract was added dropwise to the TiO_2 solution under constant stirring and kept for 1.5 hours. A white precipitate formed during the process was collected by filtration and washed with distilled water to remove impurities. The precipitate was dried in a furnace at 100°C for 24 hours, followed by heating at 200°C for 2 hours. The dried product was then sonicated in ethanol for 4 hours, yielding titanium dioxide nanoparticles (TiO_2 NPs).

Fig. 1: Synthetic route of TiO_2 NPs by using *Cichorium incubus* leaves extract

3. Results and Discussion

3.1 Green Synthesis of TiO_2 Nanoparticles

Figure 1 illustrates the eco-friendly synthesis of titanium dioxide nanoparticles (TiO_2 NPs) using *Cichorium incubus* leaves extract. Structural and chemical properties of the synthesized nanoparticles were systematically analyzed using elemental mapping, FTIR, UV-Visible spectroscopy, SEM, XRD, and EDX techniques.

3.2 Fourier transform infrared spectroscopy (FTIR)

FTIR analysis was employed to identify functional groups in *Cichorium incubus* leaf extract responsible for stabilizing TiO_2 NPs. Distinct peaks observed in the FTIR spectra confirm the successful synthesis of nanoparticles (Figure 3). The key frequencies, such as 3,466 cm^{-1}, 1,654 cm^{-1}, 1,456 cm^{-1}, and 866 cm^{-1}, correspond to free OH groups, vinyl ethers, aldehydes, and aliphatic amines, respectively.[37]–[39]

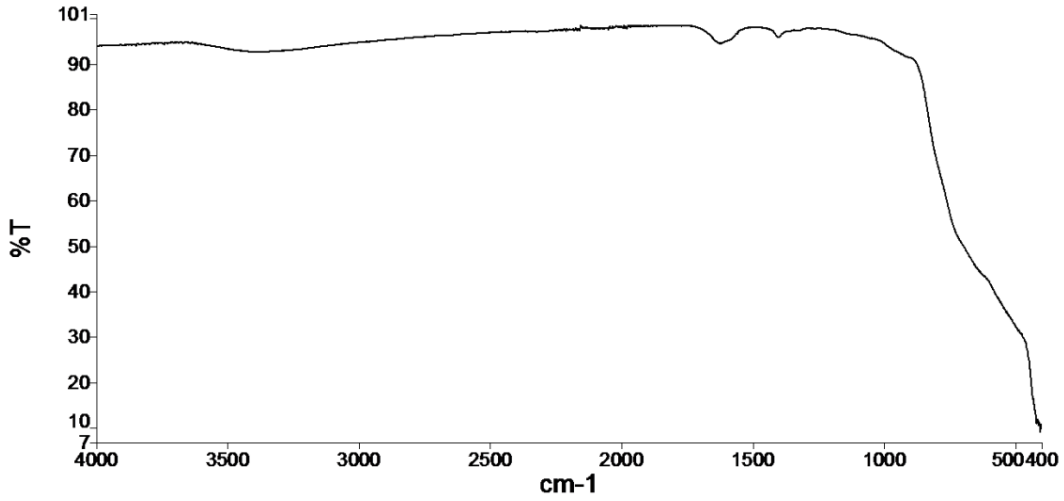

Fig. 2: FT-IR spectrum of synthesized TiO_2 NPs

3.3 X-ray Diffraction (XRD)

The average crystalline size of the green synthesized TiO_2 NPs was found to be 10 nm. Figure 1 shows the XRD pattern of TiO2 NPs obtained in the present study. After the reaction, the diffraction peaks at 2θvalues of 27.52°, 36.21°, 41.33°, 54.43°, 56.70°, and 69.16°assigned to the (110), (101), (111), (211), (220), and (301) planes of a faced center cubic lattice of titanium were obtained. The positions of principal peaks in XRD were found to bein agreement with the literature. The XRD sample shows the dominant peak of 2θ =27 which matches the 110 crystallographic plane of the rutile structure indicating that the crystal structure is predominantly rutiledominant.[40], [41] Obtained results were justified with JCPDS (Joint Committee on Powder Diffraction Standards) Card No. 78-2486. Weak peak at 30.98° was also observed and was assumed due to the orthorhombic crystalline structure. High crystalline nature of the NPs which was indicated by a sharp peak, favors the photo catalytic activity.[42]

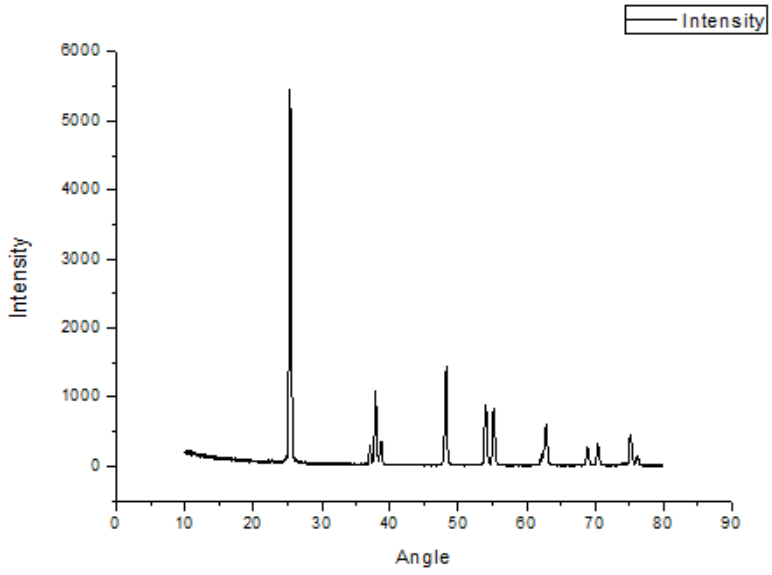

Fig. 3: X-ray diffraction study of synthesized TiO_2 NPs

3.4 UV-Vis Spectroscopy

The optical properties of TiO_2 NPs were studied using a UV-Visible spectrophotometer. The absorption spectra, shown in Figure 4, exhibit a prominent peak at 356 nm with an absorbance of 0.99, confirming nanoparticle formation. The estimated bandgap energy, calculated using the equation $Eg=hc/\lambda$ was determined to be 3.48 eV. This value highlights the photocatalytic potential of the synthesized TiO_2 NPs.[43], [44]

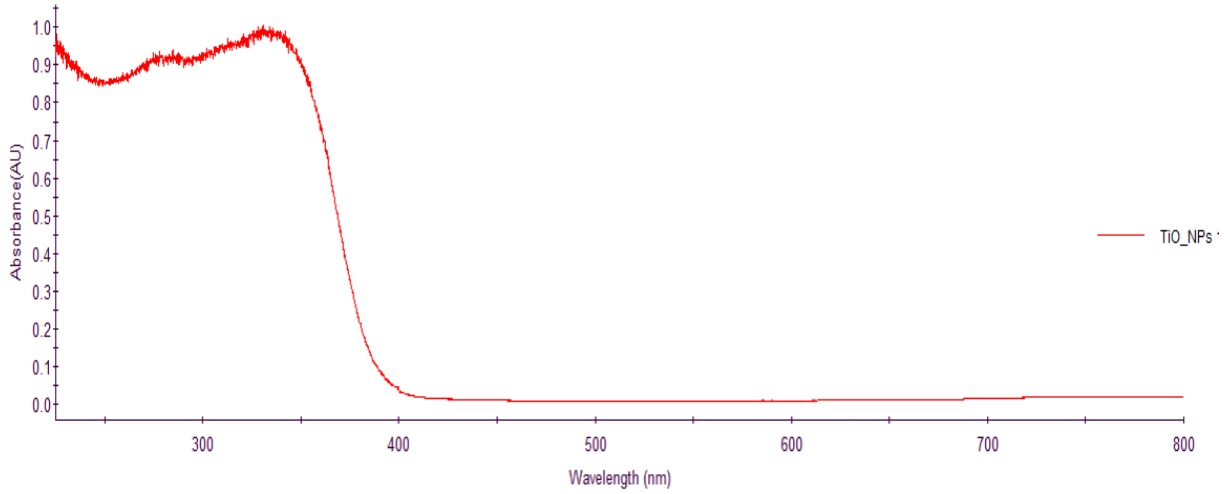

Figure 4: UV-Vis spectra of synthesized TiO_2 NPs

3.5 Scanning Electron Microscopy (SEM) and Energy Dispersive X-ray Spectroscopy (EDX)

SEM analysis (**Figure 5a–c**) revealed that the TiO_2 NPs are predominantly spherical, with minimal agglomeration and an approximate size of 100 nm. The rough surface morphology suggests an increased surface area, which enhances interaction for antimicrobial and wound-healing applications. EDX analysis (**Figure 5d**) confirmed the elemental composition of the nanoparticles, with titanium and oxygen present in a ratio close to 1:2 (38.83% Ti, 61.17% O).[45]–[47]

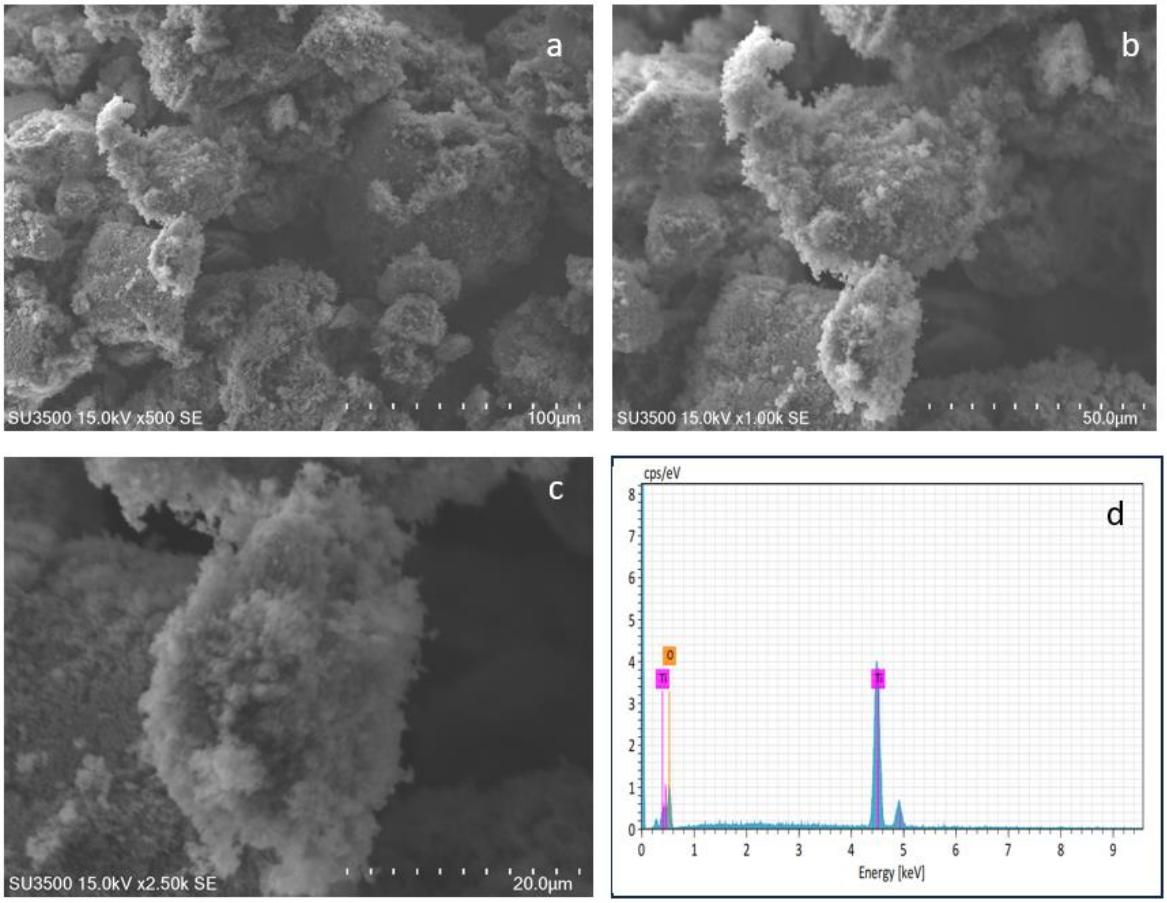

Fig. 5: a, b, c SEM images of *Cichorium Incubus* synthesized TiO_2 NPs at different magnification, d) EDX showing chemical composition and particle size distribution

3.7 Biological Activities

3.7.1 Antibacterial Activity

The antimicrobial activity of TiO_2 NPs was assessed using a zone of inhibition assay against *Escherichia coli*, *Pseudomonas aeruginosa*, and *Serratia marcescens*. No antibacterial effect was observed up to a concentration of 1,000 µg/disc. This lack of activity may be attributed to the larger particle size of the tested TiO_2 NPs compared to other reported nanoparticles, such as AgNPs, which showed higher efficacy.[48]–[51]

TABLE - 1

S. No.	Sample Id	Effective Amount	Zone at Effective Conc. (in mm)
1	Ciprofloxacin (PC)	10µg	20
2	TiO2 Nanoparticles	-	-

→ E-Coli

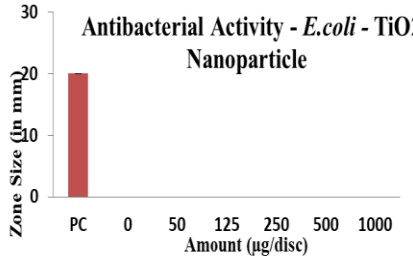

Table 2

S. No.	Sample Id	Effective Amount	Zone at Effective Conc. (in mm)
1	Ciprofloxacin (PC)	10µg	30
2	TiO2 Nanoparticle	-	-

→ S. Marcescens

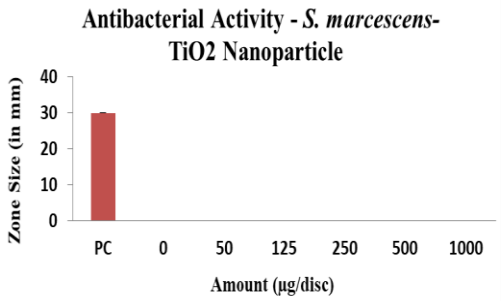

Table 3

S. No.	Sample Id	Effective Amount	Zone at Effective Conc. (in mm)
1	Ciprofloxacin (PC)	10 µg	22.66
2	TiO2 Nanoparticle	-	-

→ *P. aeruginosa*,

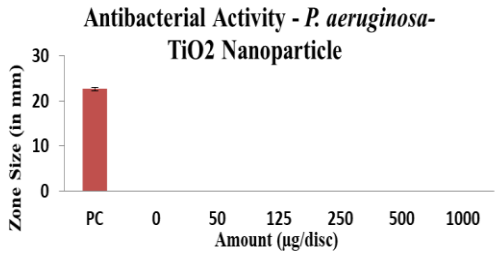

Figure 7: Antibacterial activity for bacteria: *Escherichia coli*, *Pseudomonas aeruginosa* and *S. Marcescens*

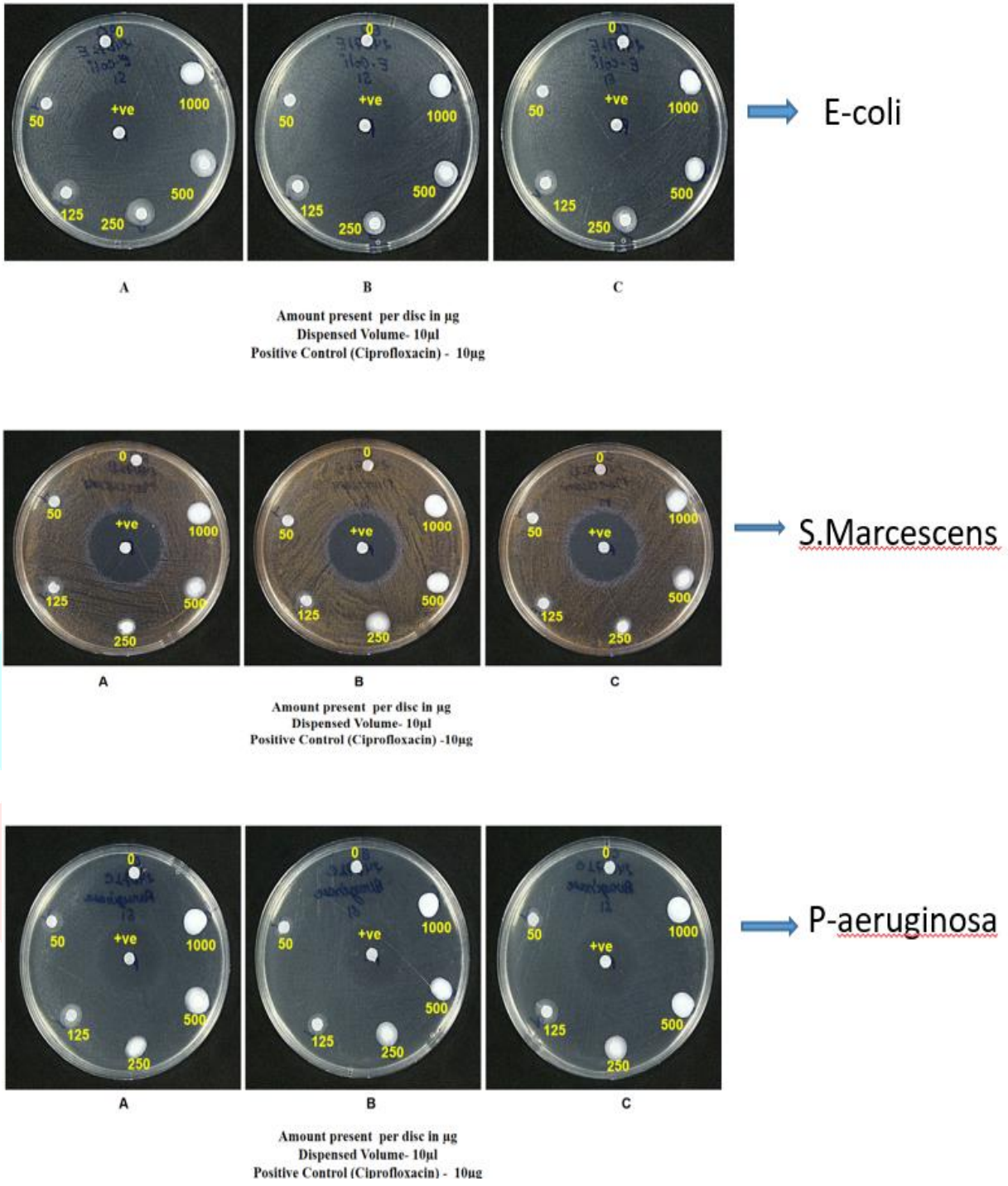

Figure 8: Antimicrobial activity of the synthesized TiO_2 NPs by disc diffusion method

3.7.2 Antifungal Activity

Similarly, the antifungal potential of TiO_2 NPs was tested against *Aspergillus niger*, *Candida parapsilosis*, *Trichoderma asperellum,* and *Candida tropicalis* using a zone of inhibition assay. No antifungal activity was observed up to 1,000 µg/disc. This result aligns with the findings for antibacterial activity, suggesting that the particle size of TiO_2 NPs may limit their antimicrobial efficacy.

TABLE - 1

S. No.	Sample Id	Effective Amount	Zone at Effective Conc. (in mm)
1	Amphotericin B (PC)	50µg	20.66
2	TiO2 Nanoparticles	-	-

➡ *C. tropicalis*

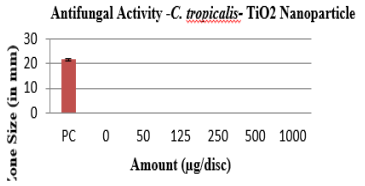

Table -2

S. No.	Sample Id	Effective Amount	Zone at Effective Conc. (in mm)
1	Amphotericin B (PC)	50 µg	23
2	TiO2 Nanoparticle	-	-

➡ C-Albicans

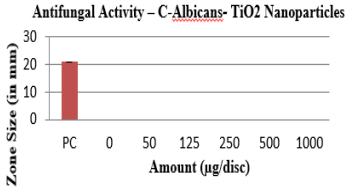

Table-3

S. No.	Sample Id	Effective Amount	Zone at Effective Conc. (in mm)
1	Amphotericin B (PC)	50µg	21
2	TiO2 Nanoparticles	-	-

➡ *A. niger*

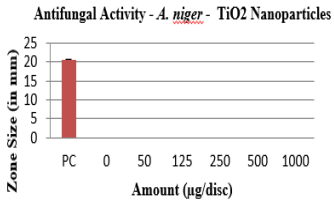

Table -4

S. No.	Sample Id	Effective Amount	Zone at Effective Conc. (in mm)
1	Amphotericin B (PC)	50 µg	21.66
2	TiO2 Nanoparticle	-	-

➡ *C. parapsilosis*

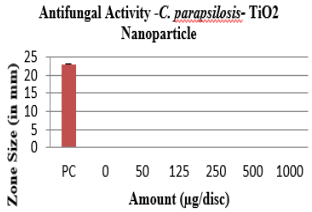

Figure 9: Antifungal activity for fungi: A. niger, C. Parapsilosis, T. Asperellum and T. C. Tropicalis

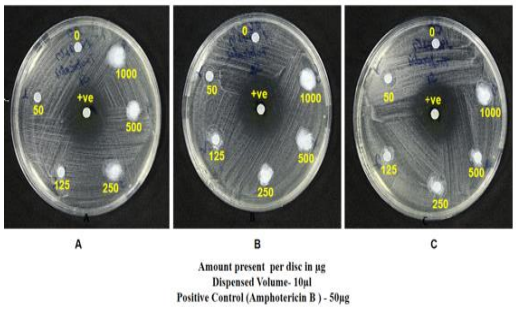

C.Tropicalis

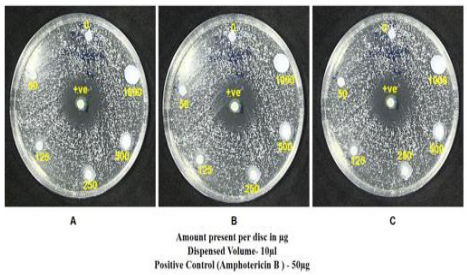

A.niger

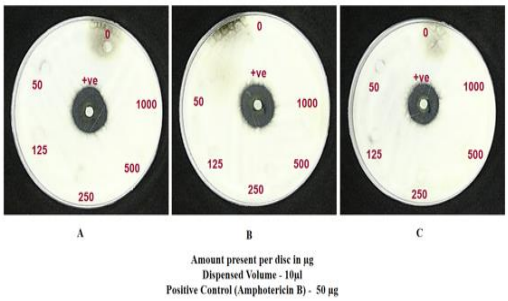

C. albicans

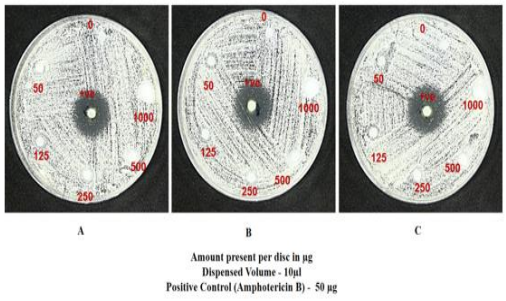

C. parapsilosa

Figure 10: Antifungal activity of the synthesized TiO_2 NPs against A. niger, C. Parapsilosis, T. Asperellum and T. C. Tropicalis fungi

3.7.3 In Vitro Cytotoxicity Evaluation

The cytotoxicity of TiO_2 NPs was evaluated using the MTT assay on L929 cell lines at concentrations of 1, 10, 50, 100, 250, 500, and 1,000 µg/mL (Figure 12). A concentration-dependent decrease in metabolic activity was observed. The IC_{50} value was determined to be 944.1 µg/mL, indicating that TiO_2 NPs exhibit mild cytotoxicity at higher concentrations. Microscopic images (Figure 11) illustrate the changes in cell morphology and viability at varying concentrations.

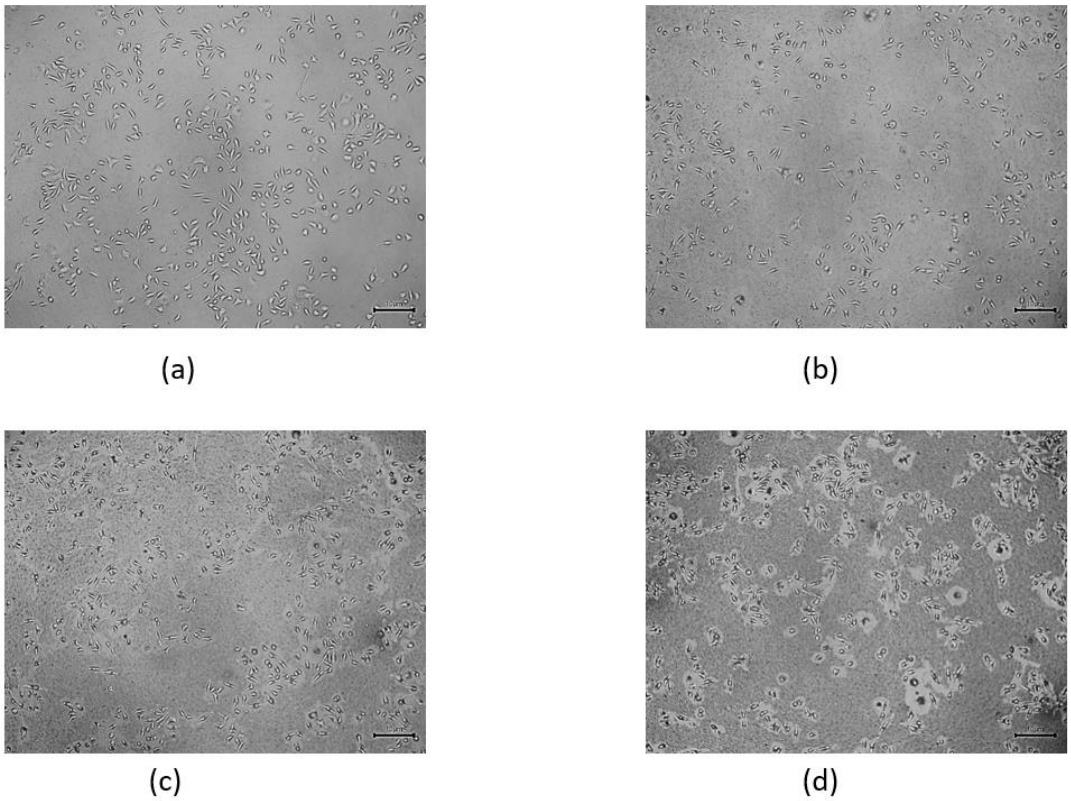

Figure 11: Microscopic images of L929 cell lines after treatment with different concentrations of sample (a) at 10 µg/ml (b) at 100µg/ml (c) at 250 µg/ml (d) at 500 µg/ml

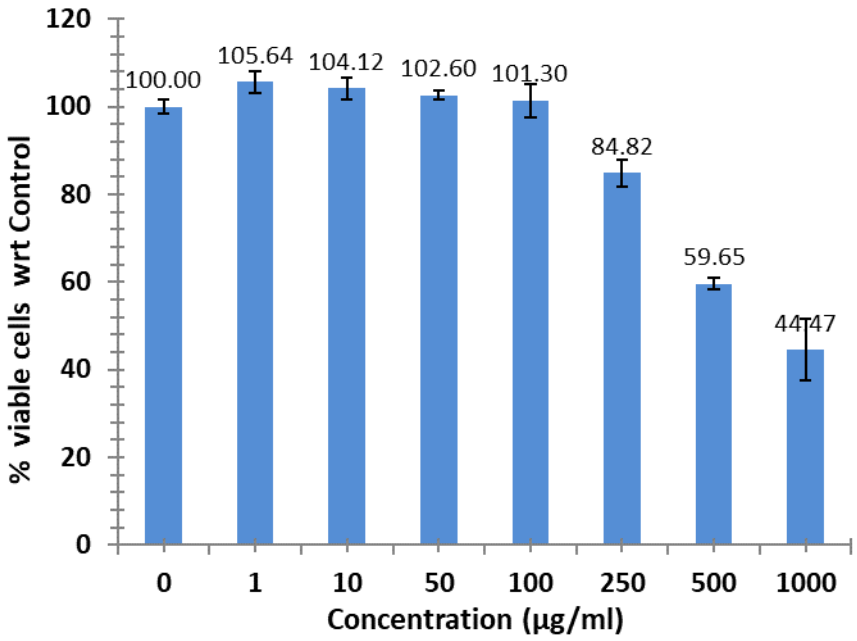

Fig. 12: Cytotoxicity levels at different concentration of samples

3.7.4 Wound Healing Assay

The wound healing potential of TiO_2 NPs was assessed using a scratch assay on L929 cell lines (Figure 13). Treated cells exhibited enhanced wound closure compared to the control group. The healing rate was measured after 24 hours, showing 42.17% closure for the control group and 57.44% closure for cells treated with 236.02 µg/mL of TiO_2 NPs (Figure 14). These findings suggest the potential application of TiO_2 NPs in promoting wound healing, warranting further investigation.

3.7.4 Wound Healing Assay for L929 Cell Line

This study evaluated the wound healing potential of titanium dioxide nanoparticles (TiO_2 NPs) synthesized using *Cichorium incubus* leaf extract on L929 cell lines. The assay was performed by creating a scratch wound and treating the cells with varying concentrations of the nanoparticles, as shown in Figure 13. The metabolic activity of the L929 cells after a 24-hour incubation period was assessed using the MTT assay, which provided insights into the wound healing capabilities of the TiO_2 NPs.

The scratched area was measured and considered 100% at zero hours, and the extent of healing was quantified after 24 hours of treatment. As depicted in Figure 14, untreated control cells exhibited a healing rate of 42.17%. In contrast, cells treated with TiO_2 NPs at a concentration of 236.02 µg/mL demonstrated enhanced wound closure, with a healing rate of 57.44%. These results highlight the potential of TiO_2 NPs in promoting wound healing, suggesting further exploration for their applications in regenerative medicine

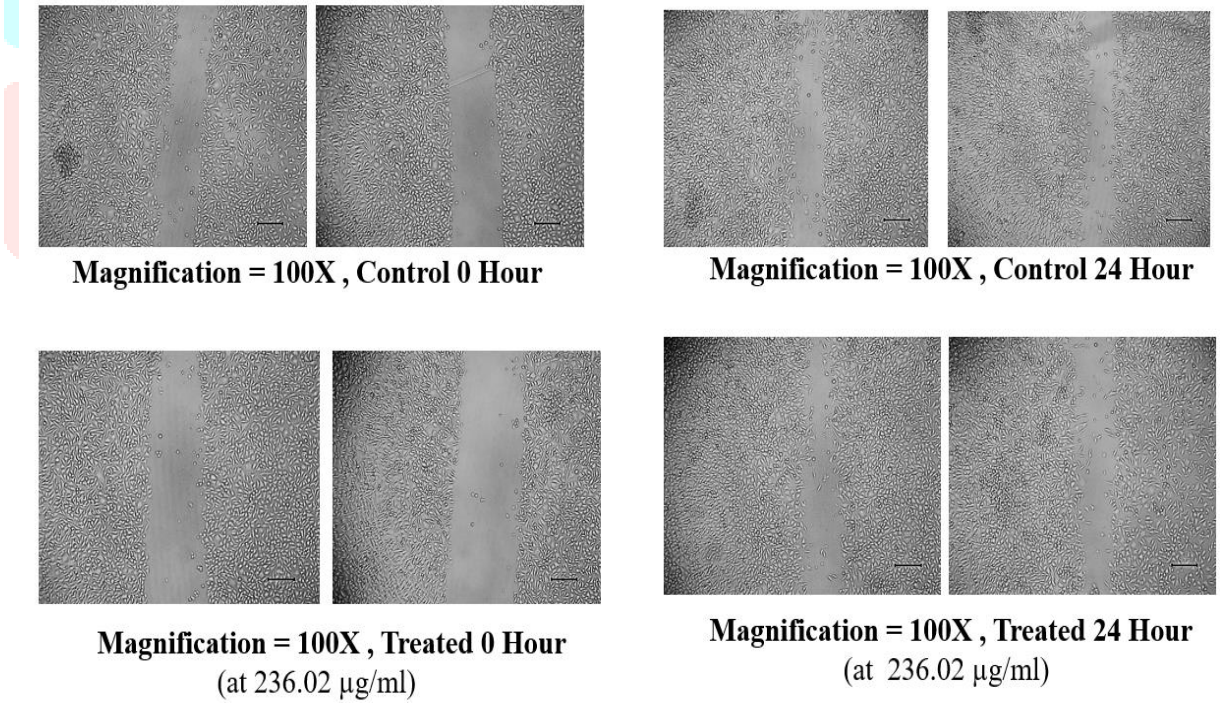

Fig. 13: Microscopic images of L929 cell lines control and after treatmentat zero hour and 24 hours

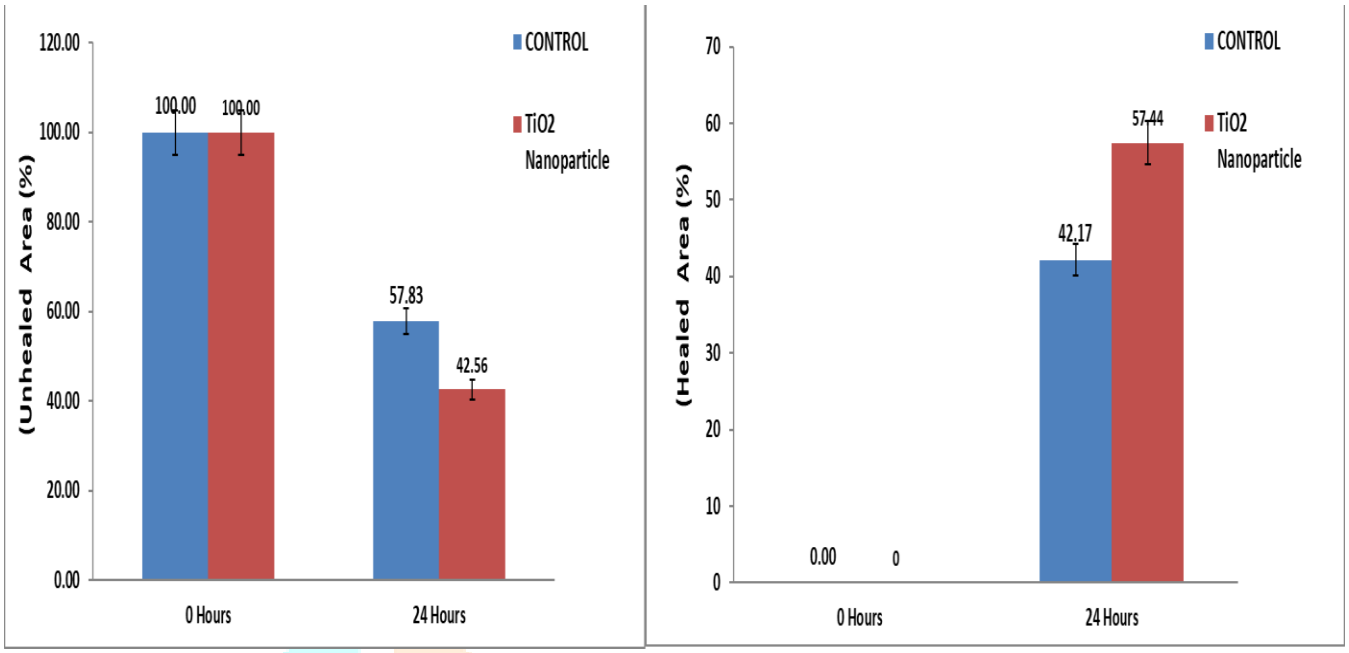

Fig. 14: Healed and unhealed area was estimated in percentage at different concentration of samples

4. Conclusion

Titanium dioxide nanoparticles (TiO_2 NPs) were synthesized using an eco-friendly and cost-effective method involving *Cichorium incubus* leaf extract and titanium dioxide solution. Comprehensive characterization using FTIR, UV-Vis spectroscopy, XRD, SEM, and EDX confirmed the successful synthesis of TiO_2 NPs. FTIR analysis revealed the functional groups involved in nanoparticle stabilization, UV-Vis spectroscopy demonstrated characteristic absorption peaks indicative of nanoparticle formation, SEM provided insights into surface morphology and size distribution, and EDX confirmed the elemental composition.

Biological evaluation showed that TiO_2 NPs lacked significant antibacterial and antifungal activity at concentrations up to 1000 µg/well. However, in vitro cytotoxicity studies on L929 cell lines using the MTT assay determined an IC_{50} value, indicating 50% inhibition of cell viability at a specific concentration. Furthermore, the wound healing assay revealed promising results, with the treated group showing a healing rate of 236.02 µg/mL after 24 hours compared to 42.17% in the control group. These findings suggest potential applications of TiO_2 NPs in wound healing, warranting further studies to explore and optimize their biological properties.

5. List of Abbreviations

1. **TiO_2 NPs** - Titanium dioxide nanoparticles
2. **FTIR** - Fourier transform infrared spectroscopy
3. **EDX** - Energy dispersive X-ray spectroscopy
4. **SEM** - Scanning Electron Microscopy
5. **UV-Vis** - Ultraviolet-Visible Spectroscopy
6. ***E. coli* (-ve)** - *Escherichia coli* (negative)
7. ***S. marcescens* (-ve)** - *Serratia marcescens* (negative)
8. ***P. aeruginosa* (-ve)** - *Pseudomonas aeruginosa* (negative)
9. ***C. parapsilosis*** - *Candida parapsilosis*
10. ***T. asperellum*** - *Trichoderma asperellum*
11. ***C. tropicalis*** - *Candida tropicalis*
12. ***A. niger*** - *Aspergillus niger*
13. ***C. albicans*** - *Candida albicans*

14. **L929 cell line** - Mouse fibroblast L929 cells

6. Acknowledgements

The authors extend their heartfelt gratitude to the Chemistry Laboratory at Starex University, Gurugram, for their unwavering support and provision of essential facilities and chemicals, which were pivotal in synthesizing the sample materials. We also sincerely appreciate the Centre for Advanced Materials and Devices at BML Munjal University for their expertise and resources in characterizing the samples. Their assistance played a critical role in ensuring a comprehensive analysis and validation of our research findings.

Special thanks go to Aakaar Biotechnologies Private Limited for conducting the antibacterial, antifungal, in vitro cytotoxicity, and wound healing assays. Their contribution was vital in evaluating the biological efficacy of the synthesized nanoparticles, significantly enhancing the scope and impact of our research.

The collaborative efforts and support of these institutions have been instrumental in advancing the quality and depth of our study, allowing us to achieve our scientific objectives and contribute meaningfully to the field.

References

[1] S. P. Goutam, G. Saxena, V. Singh, A. K. Yadav, R. N. Bharagava, and K. B. Thapa, "Green synthesis of TiO2 nanoparticles using leaf extract of Jatropha curcas L. for photocatalytic degradation of tannery wastewater," *Chem. Eng. J.*, vol. 336, pp. 386–396, 2018, doi: 10.1016/j.cej.2017.12.029.

[2] F. Behzad, S. M. Naghib, M. Amin, S. N. Tabatabaei, Y. Zare, and K. Y. Rhee, "An overview of the plant-mediated green synthesis of noble metal nanoparticles for antibacterial applications," *J. Ind. Eng. Chem.*, 2020, doi: 10.1016/j.jiec.2020.12.005.

[3] P. Velmurugan *et al.*, "Phytosynthesis of silver nanoparticles by Prunus yedoensis leaf extract and their antimicrobial activity," *Mater. Lett.*, vol. 138, pp. 272–275, 2015, doi: 10.1016/j.matlet.2014.09.136.

[4] S. Kota, P. Dumpala, R. K. Anantha, M. K. Verma, and S. Kandepu, "Evaluation of therapeutic potential of the silver/silver chloride nanoparticles synthesized with the aqueous leaf extract of Rumex acetosa," *Sci. Rep.*, vol. 7, no. 1, pp. 1–11, 2017, doi: 10.1038/s41598-017-11853-2.

[5] A. S. Eltaweil, M. Fawzy, M. Hosny, E. M. Abd El-Monaem, T. M. Tamer, and A. M. Omer, "Green synthesis of platinum nanoparticles using Atriplex halimus leaves for potential antimicrobial, antioxidant, and catalytic applications," *Arabian Journal of Chemistry*, vol. 15, no. 1. 2022. doi: 10.1016/j.arabjc.2021.103517.

[6] B. Xia *et al.*, "Ocean acidification increases the toxic effects of TiO2 nanoparticles on the marine microalga Chlorella vulgaris," *J. Hazard. Mater.*, vol. 346, pp. 1–9, 2018, doi: 10.1016/j.jhazmat.2017.12.017.

[7] A. A. A. Aljabali *et al.*, "Synthesis of gold nanoparticles using leaf extract of ziziphus zizyphus and their antimicrobial activity," *Nanomaterials*, vol. 8, no. 3, pp. 1–15, 2018, doi: 10.3390/nano8030174.

[8] R. Moeinzadeh, M. Hekmati, N. Azizi, M. Qomi, and D. Esmaeili, "Investigation of the antibacterial activity of phytosynthesized ZnO nanoparticles using H. perforatum extract," *Chem. Rev. Lett.*, vol. 7, no. 2, pp. 185–200, 2024, doi: 10.22034/crl.2024.435875.1281.

[9] V. Mohammadzadeh *et al.*, "Applications of plant-based nanoparticles in nanomedicine: A review," *Sustain. Chem. Pharm.*, vol. 25, p. 100606, 2022, doi: https://doi.org/10.1016/j.scp.2022.100606.

[10] P. C. Nagajyothi, S. V. Prabhakar Vattikuti, K. C. Devarayapalli, K. Yoo, J. Shim, and T. V. M. Sreekanth, "Green synthesis: Photocatalytic degradation of textile dyes using metal and metal oxide nanoparticles-latest trends and advancements," *Crit. Rev. Environ. Sci. Technol.*, vol. 50, no. 24, pp. 2617–2723, 2020, doi: 10.1080/10643389.2019.1705103.

[11] S. M. Mousavi *et al.*, "Green synthesis of silver nanoparticles toward bio and medical applications:

review study," *Artificial Cells, Nanomedicine and Biotechnology*, vol. 46, no. sup3. pp. S855–S872, 2018. doi: 10.1080/21691401.2018.1517769.

[12] J. Singh, T. Dutta, K. H. Kim, M. Rawat, P. Samddar, and P. Kumar, "'Green' synthesis of metals and their oxide nanoparticles: Applications for environmental remediation," *J. Nanobiotechnology*, vol. 16, no. 1, pp. 1–24, 2018, doi: 10.1186/s12951-018-0408-4.

[13] N. A. Mirgane, V. S. Shivankar, S. B. Kotwal, G. C. Wadhawa, and M. C. Sonawale, "Waste pericarp of ananas comosus in green synthesis zinc oxide nanoparticles and their application in waste water treatment," *Mater. Today Proc.*, vol. 37, no. Part 2, pp. 886–889, 2020, doi: 10.1016/j.matpr.2020.06.045.

[14] R. Hao, D. Li, J. Zhang, and T. Jiao, "Green synthesis of iron nanoparticles using green tea and its removal of hexavalent chromium," *Nanomaterials*, vol. 11, no. 3, pp. 1–13, 2021, doi: 10.3390/nano11030650.

[15] J. K. Patra *et al.*, "Nano based drug delivery systems: Recent developments and future prospects 10 Technology 1007 Nanotechnology 03 Chemical Sciences 0306 Physical Chemistry (incl. Structural) 03 Chemical Sciences 0303 Macromolecular and Materials Chemistry 11 Medical and He," *J. Nanobiotechnology*, vol. 16, no. 1, pp. 1–33, 2018, doi: 10.1186/s12951-018-0392-8.

[16] É. S. Almeida, D. de Oliveira, and D. Hotza, "Properties and Applications of Morinda citrifolia (Noni): A Review," *Compr. Rev. Food Sci. Food Saf.*, vol. 18, pp. 883–909, 2019, doi: 10.1111/1541-4337.12456.

[17] N. M. Alabdallah and M. Hasan, "Saudi Journal of Biological Sciences Plant-based green synthesis of silver nanoparticles and its effective role in abiotic stress tolerance in crop plants," *Saudi J. Biol. Sci.*, no. xxxx, 2021, doi: 10.1016/j.sjbs.2021.05.081.

[18] K. Z. Kolo, N. C. Nwokem, and S. E. Abechi, "Green Synthesis of Iron Oxide Nanoparticle Using Funaria hygrometrica Extract, and the Study of Its Antimicrobial Activities," *J. Chem. Lett.*, vol. 4, no. 4, pp. 222–231, 2024.

[19] M. L. Birsa and L. G. Sarbu, "Health Benefits of Key Constituents in Cichorium intybus L.," *Nutrients*, vol. 15, no. 6, 2023, doi: 10.3390/nu15061322.

[20] M. Panwar and D. Rawat, "Traditional Uses of Cichorium Intybus and its Medicinal Importance for Health," *Jclmm*, vol. 2, no. 11, pp. 1586–1602, 2023, [Online]. Available: https://www.researchgate.net/figure/Historical-overview-of-chicory-use-An-overview-is-presented-of-the-

[21] Ł. Duda *et al.*, "Medicinal Use of Chicory (Cichorium intybus L.)," *Sci. Pharm.*, vol. 92, no. 2, pp. 1–17, 2024, doi: 10.3390/scipharm92020031.

[22] K. Janda, I. Gutowska, M. Geszke-Moritz, and K. Jakubczyk, "The common cichory (Cichorium intybus l.) as a source of extracts with health-promoting properties—a review," *Molecules*, vol. 26, no. 6, pp. 1–14, 2021, doi: 10.3390/molecules26061814.

[23] R. Jin, L. Luo, and J. Zheng, "The Trinity of Skin: Skin Homeostasis as a Neuro–Endocrine–Immune Organ," *Life*, vol. 12, no. 5, pp. 1–11, 2022, doi: 10.3390/life12050725.

[24] A. Al Mamun, C. Shao, P. Geng, S. Wang, and J. Xiao, "Recent advances in molecular mechanisms of skin wound healing and its treatments," *Front. Immunol.*, vol. 15, no. May, pp. 1–29, 2024, doi: 10.3389/fimmu.2024.1395479.

[25] P. Kumar and V. Kumar, "Diabetic Wound Healing: Navigating Physiology, Advancements and Research Frontiers," *J. Diabetes Res. Rev. Reports*, no. July, pp. 1–11, 2024, doi: 10.47363/jdrr/2024(6)181.

[26] P. David, S. Singh, and R. Ankar, "A Comprehensive Overview of Skin Complications in Diabetes and Their Prevention," *Cureus*, vol. 15, no. 5, 2023, doi: 10.7759/cureus.38961.

[27] M. Chakravarthy, "Antimicrobial Resistance and Stewardship," *Hosp. Infect. Control Guidel. Princ.*

Pract., no. August, pp. 101–101, 2012, doi: 10.5005/jp/books/11657_9.

[28] D. R. Long, A. Cifu, S. J. Salipante, R. G. Sawyer, K. MacHutta, and J. C. Alverdy, "Preventing Surgical Site Infections in the Era of Escalating Antibiotic Resistance and Antibiotic Stewardship," *JAMA Surg.*, vol. 159, no. 8, pp. 949–956, 2024, doi: 10.1001/jamasurg.2024.0429.

[29] Aliu Olalekan Olatunji, Janet Aderonke Olaboye, Chukwudi Cosmos Maha, Tolulope Olagoke Kolawole, and Samira Abdul, "Next-Generation strategies to combat antimicrobial resistance: Integrating genomics, CRISPR, and novel therapeutics for effective treatment," *Eng. Sci. Technol. J.*, vol. 5, no. 7, pp. 2284–2303, 2024, doi: 10.51594/estj.v5i7.1344.

[30] C. de la Fuente-Nunez, A. Cesaro, and R. E. W. Hancock, "Antibiotic failure: Beyond antimicrobial resistance," *Drug Resist. Updat.*, vol. 71, pp. 1–27, 2023, doi: 10.1016/j.drup.2023.101012.

[31] Y. Wang, M. Zhang, Z. Yan, S. Ji, S. Xiao, and J. Gao, "Metal nanoparticle hybrid hydrogels: The state-of-the-art of combining hard and soft materials to promote wound healing," *Theranostics*, vol. 14, no. 4, pp. 1534–1560, 2024, doi: 10.7150/thno.91829.

[32] S. N. Nandhini *et al.*, "Recent advances in green synthesized nanoparticles for bactericidal and wound healing applications," *Heliyon*, vol. 9, no. 2, p. e13128, 2023, doi: 10.1016/j.heliyon.2023.e13128.

[33] S. Ali, S. Sulaiman, A. Khan, M. R. Khan, and R. Khan, "Green synthesized silver nanoparticles (AgNPs) from Parrotiopsis jacquemontiana (Decne) Rehder leaf extract and its biological activities," *Microscopy Research and Technique*, vol. 85, no. 1. pp. 28–43, 2022. doi: 10.1002/jemt.23882.

[34] R. Sarah, B. Tabassum, N. Idrees, and M. K. Hussain, "Bio-active Compounds Isolated from Neem Tree and Their Applications," in *Natural Bio-active Compounds: Volume 1: Production and Applications*, M. S. Akhtar, M. K. Swamy, and U. R. Sinniah, Eds., Singapore: Springer Singapore, 2019, pp. 509–528. doi: 10.1007/978-981-13-7154-7_17.

[35] P. D. Kilmer, "Review Article: Review Article," *Journalism*, vol. 11, no. 3, pp. 369–373, 2010, doi: 10.1177/1461444810365020.

[36] A. Ghareeb, A. Fouda, R. M. Kishk, and W. M. El Kazzaz, "Unlocking the potential of titanium dioxide nanoparticles: an insight into green synthesis, optimizations, characterizations, and multifunctional applications," *Microb. Cell Fact.*, vol. 23, no. 1, 2024, doi: 10.1186/s12934-024-02609-5.

[37] S. Dzwigaj *et al.*, "DFT makes the morphologies of anatase-TiO2 nanoparticles visible to IR spectroscopy," *J. Catal.*, vol. 236, no. 2, pp. 245–250, 2005, doi: 10.1016/j.jcat.2005.09.034.

[38] A. J. Maira, J. M. Coronado, V. Augugliaro, K. L. Yeung, J. C. Conesa, and J. Soria, "Fourier transform infrared study of the performance of nanostructured TiO2 particles for the photocatalytic oxidation of gaseous toluene," *J. Catal.*, vol. 202, no. 2, pp. 413–420, 2001, doi: 10.1006/jcat.2001.3301.

[39] J. Y. Zhang, I. W. Boyd, B. J. O'Sullivan, P. K. Hurley, P. V. Kelly, and J. P. Sénateur, "Nanocrystalline TiO2 films studied by optical, XRD and FTIR spectroscopy," *J. Non. Cryst. Solids*, vol. 303, no. 1, pp. 134–138, 2002, doi: 10.1016/S0022-3093(02)00973-0.

[40] D. K. De Mukhopadhyay, "Pharmacokinetic Study of Novel Drug Delivery Systems for Insulin Administration in Diabetic Patients," *African J. Biomed. Res.*, vol. 27, no. 3, pp. 217–225, 2024, doi: 10.53555/za3b5j84.

[41] L. Abdulazeem, B. H. H. AL-Amiedi, H. A. Alrubaei, and Y. H. AL-Mawlah, "Titanium dioxide nanoparticles as antibacterial agents against some pathogenic bacteria," *Drug Invent. Today*, vol. 12, no. 5, pp. 963–967, 2019.

[42] M. A. Irshad *et al.*, "Synthesis, characterization and advanced sustainable applications of titanium dioxide nanoparticles: A review," *Ecotoxicol. Environ. Saf.*, vol. 212, p. 111978, 2021, doi: 10.1016/j.ecoenv.2021.111978.

[43] M. Alavi and N. Karimi, "Characterization, antibacterial, total antioxidant, scavenging, reducing power

and ion chelating activities of green synthesized silver, copper and titanium dioxide nanoparticles using Artemisia haussknechtii leaf extract," *Artif. Cells, Nanomedicine Biotechnol.*, vol. 46, no. 8, pp. 2066–2081, 2018, doi: 10.1080/21691401.2017.1408121.

[44] S. S. Ghani and F. Ghani, "Green synthesis and antibacterial activity of cobalt nanoparticle from Calotropis gigantae," *J. Mex. Chem. Soc.*, vol. 64, no. 2, pp. 64–73, 2020, doi: 10.29356/jmcs.v64i2.1118.

[45] M. M. Viana, V. F. Soares, and N. D. S. Mohallem, "Synthesis and characterization of TiO2 nanoparticles," *Ceram. Int.*, vol. 36, no. 7, pp. 2047–2053, 2010, doi: 10.1016/j.ceramint.2010.04.006.

[46] *et al.*, "Synthesis of nickel nanoparticles by sol-gel method and their characterization," *Open J. Chem.*, vol. 2, no. 1, pp. 16–20, 2019, doi: 10.30538/psrp-ojc2019.0009.

[47] R. Vijayalakshmi and V. Rajendran, "Synthesis and characterization of nano-TiO2 via different methods," *Sch. Res. Libr.*, vol. 4, no. 2, pp. 1183–1190, 2012, doi: 10.11648/j.nano.20140201.11.

[48] B. Singha, V. Singh, and V. Soni, "Alternative therapeutics to control antimicrobial resistance: a general perspective," *Front. Drug Discov.*, vol. 4, no. July, pp. 1–17, 2024, doi: 10.3389/fddsv.2024.1385460.

[49] T. Bezrodna, G. Puchkovska, V. Shymanovska, J. Baran, and H. Ratajczak, "IR-analysis of H-bonded H2O on the pure TiO2 surface," *J. Mol. Struct.*, vol. 700, no. 1–3, pp. 175–181, 2004, doi: 10.1016/j.molstruc.2003.12.057.

[50] A. A. Fadda, R. Rabie, and H. A. Etman, "Synthesis and Evaluation of the Antimicrobial Activity," vol. 32, no. 3, pp. 451–458, 2014.

[51] M. Kovalskyi, W. Duczmal, M. Oleksiuk, A. Skomorovskyi, and Z. Berezivskyy, "Renewable Energy Sources in the Context of Emissions Reduction: Geographical Aspects and Challenges for Sustainable Development," *African J. Appl. Res.*, vol. 10, no. 1, pp. 374–386, 2024, doi: 10.26437/ajar.v10i1.709.